The transcription factors TCF1 and LEF1 drive B-1a cell development, self-renewal, and regulatory function.

Carola Vinuesa (carola.vinuesa@crick.ac.uk)
Francis Crick Institute https://orcid.org/0000-0001-9799-0298

Qian Shen
Francis Crick Institute

Hao Wang
Francis Crick Institute

Xiangpeng Meng
Division of Immunology and Infectious Disease, John Curtin School of Medical Research, Australian National University,

Jonathan Roco
The John Curtin School of Medical Research

Michael Battaglia
Department of Biochemistry, State University of New York at Buffalo

Zhi-Ping Feng
The Australian National University https://orcid.org/0000-0002-6627-5934

Probir Chakravarty
The Francis Crick Institute

Pablo Canete
ANU, John Curtin School of Medical Research

Paula Gonzalez-Figueroa
ANU, John Curtin School of Medical Research

Yaoyuan Zhang
Division of Immunology and Infectious Disease, John Curtin School of Medical Research, Australian National University

Hai-Hui Xue
Hackensack University Medical Center https://orcid.org/0000-0002-9163-7669

Lee Garrett-Sinha
State University of New York at Buffalo

Biological Sciences - Article

Keywords:

Posted Date: January 17th, 2024

DOI: https://doi.org/10.21203/rs.3.rs-3855081/v1

Additional Declarations: There is **NO** Competing Interest.

Abstract

B-1 cells are abundant in peritoneal and pleural cavities and produce natural and microbial-induced IgM and IgA1–4.CD5+ B-1 cells known as “B-1a” represent the largest source of B cell-derived IL-105,6, an important regulator of inflammation and autoimmunity7. Unlike conventional B cells that are produced daily in the bone marrow, B-1a cells are predominantly generated from foetal precursors and maintained by self-renewal8 but the molecular mechanisms that underpin this stem cell-like property and their regulatory potential are poorly understood. Here we show that both mouse and human B-1a cells express high amounts of TCF1 and LEF1 and these transcription factors drive their formation and self-renewal promoting oxidative and fatty acid metabolism. Deficiency of TCF1/LEF1 in B-1a cells leads to downregulation of Ets1 and Myc targets, and severely compromises their maintenance over time. TCF1 and LEF1 are also essential for IL-10 and PD-L1 expression upon B-1 cell activation and repression of CNS inflammation. TCF1/LEF1 mediate the emergence of a mixed cell progeny at the third B-1 cell division including a stem-cell-like population. B-1 cells lacking TCF1/LEF1 continue proliferating and acquire an exhausted phenotype reminiscent of age-associated B cells. These findings identify a transcriptional program that links stemness with regulatory potential in B-1a cells.

Introduction

B-1a cells play important anti-inflammatory roles: their antibodies recognise components of bacterial and senescent red blood cell membranes, as well as apoptotic cells and oxidized lipids and help prevent inflammation and tissue damage. Upon stimulation, peritoneal B-1a cells migrate to the spleen where they secrete higher amounts of protective antibodies and cytokines [9]. Peritoneal B-1a cells and their splenic $CD5^+$ offspring are also potent repressors of innate and adaptive autoreactive and inflammatory immune responses including experimental allergic encephalomyelitis (EAE), largely due to their ability to produce IL-10 [10–13]**.** B-1a cells are also the normal counterpart of the malignant B cells that cause chronic lymphocytic leukemia, the most common form of adult leukemia, which is also known to secrete IL-10[14,15]. B-1a cells have a restricted BCR repertoire [16] and their differentiation is largely instructed by BCR signal strength and self-reactivity[17,18]. The fact that germline-encoded BCR specificity is selected and maintained in the absence of external antigen and T cell help has led to the proposal that B-1 cells are in essence “natural memory” cells [19]. Indeed, one of the cardinal features of B-1 cells is that they can persist through adulthood likely due to their capacity to self-renew, a process that requires sustained but limited proliferation to maintain a stable cell pool over time [20,21]. B-1a cells in the peritoneal cavity not only have slow turnover rates compared to B-2 cells [22,23], but also can completely reconstitute host tissues lacking these cells after adoptive transfer and persist for many months with little contribution from host-derived cells [24]. To date, the mechanism underpinning B-1a self-renewal remains unknown. Here we show that TCF1 and LEF1 – known to confer stem-cell like properties in various cell types including $CD8^+$ T cells [25] - play essential roles in controlling self-renewal of B-1a cells via controlling a Myc-regulated program, and importantly, driving IL-10 production and the regulatory ability of B-1a cells.

TCF1 and LEF1 are essential for B-1a cell development.

To understand the transcriptional program governing B-1 cell homeostasis we performed single-cell RNA sequencing (scRNA-seq) on sorted peritoneal B cells from adult mice. Immunoglobulin genes were removed from the unsupervised analysis to avoid clonal BCRs determining the clusters. The determinants of the two major subclusters were *Cd5* and *Fcer2a* (encoding for CD23, expressed highly in recirculating follicular B cells). *Tcf7 (encoding* TCF1)[26] was expressed in the *Cd5* subcluster, together with *Bhlhe41*, both known to be regulators of B-1a cell development [27] (Fig. 1a and Extended Fig. 1a). *Tcf7* was also most highly expressed in both peritoneal cavity and spleen B-1 cell subsets according to Immgen (Extended Fig.1b) and protein detection by flow cytometry (Fig.1b-d). LEF1 is a transcriptional factor (TF) that shares overlapping functions with TCF1 in many biological processes [28,29]. While *Lef1* mRNA was only highly expressed in splenic B-1a cells and not in peritoneal cavity B-1a cells (Extended Fig.1a), both TCF1 and LEF1 protein expression were highest in B-1 cells from both spleen and peritoneal cavity B-1 cells compared with B2 subsets (Fig. 1b-d). Analysis of bone marrow cells revealed that TCF1 and LEF1 are expressed from the earliest stages of B-1 cell development, being already detected in pro-B cells that give rise to both B-1 and B2 cell progenitors, as well as in B-1 progenitor cells (B-1P) (Extended Figure.1c). High TCF1 and LEF1 expression was also a feature of human B-1a cells from tonsil and peripheral blood (Extended Fig.1d).

Having identified selective high expression of TCF1 and LEF1 in B-1 cells, we next sought to determine the role of these TFs in B-1 cell biology. To generate mice conditionally lacking these TFs only in B cells, we crossed *Tcf7*-floxed and *Lef1*-floxed mice to mice expressing Cre under the control of the *Mb1* promoter, which is expressed from the early pro-B cell stage [30]. B-1a cells were decreased in peritoneal cavity and spleen of mice doubly deficient for both TCF1 and LEF1 ($Tcf7^{flox/flox}$.$Lef1^{flox/flox}$.Cre^{Mb1} mice, abbreviated as $TCF1^{\Delta}LEF1^{\Delta}$) compared to wild type controls - $Tcf7^{flox/+}$.$Lef1^{flox/+}$.Cre^{Mb1} or $Tcf7^{flox/flox}$.$Lef1^{flox/flox}$ (abbreviated as $TCF1^{WT}LEF1^{WT}$). Whilst mice with single LEF1 deficiency ($Lef1^{flox/flox}$.Cre^{Mb1} ($LEF1^{\Delta}$)) also had decreased B-1a cells in both peritoneal cavity and spleen, deficiency of TCF1 alone ($Tcf7^{flox/flox}$.Cre^{Mb1}) only decreased splenic B-1a cells. This suggests that LEF1 may be sufficient for formation and/or maintenance of peritoneal B-1a cells but TCF1 is also required for their maintenance in secondary lymphoid tissues once they leave the peritoneal cavity. By contrast, neither TCF1 nor LEF1 altered the frequency of peritoneal B-1b or splenic follicular B-2 cells (Fig. 1e, f and Extended Fig.1e). B-2 cell development, including formation of B-1 progenitor cells in the bone marrow was unaffected in $TCF1^{\Delta}LEF1^{\Delta}$ mice (Extended Fig.1f).

We next sought to establish whether TCF1 and LEF1 are required for development of foetal liver and/or bone marrow-derived B-1a cells. For this, sub-lethally irradiated $Rag1^{-/-}$ mice were reconstituted with either E14.5 foetal liver cells or adult bone marrow cells from mice sufficient or deficient in TCF1 and LEF1. B-1a cells decreased by 70% in mice receiving $TCF1^{\Delta}LEF1^{\Delta}$ foetal liver cells compared to recipients of wild-type cells, while the fractions of peritoneal B-1b, bone marrow proB, preB, B-1P and immature were comparable between the two groups; only a small (~20%) reduction was observed in splenic follicular

recirculating B cells (Fig. 1g and Extended Fig. 1g). Similar results were obtained in recipients of bone marrow cells, although the reduction in B-1a cells was less marked (Fig. 1g). Together these results suggest TCF1 and LEF1 play an important role in B-1a cell development.

Next, we evaluated the consequence of combined TCF1 and LEF1 deficiency in B-1a cell development from gestation through adulthood. B-1 progenitors (B-1P), identified as $Lin^{-}CD93^{+}IgM^{-}CD19^{+}B220^{neg\text{-}lo}$, can differentiate into both B-1a and B-1b cells or mature in the spleen through a transitional (TrB-1a) cell stage [31]. B-1P peak during late gestation and decline after birth as B-2 development is established in adult bone marrow (Fig. 2a) [32]. TCF1 and LEF1 deficiency resulted in an increased frequency of B-1P cells in E18.5 foetal liver and neonatal (days 1, 3 and 9) bone marrow (Fig. 2b and Extended Fig. 2a&c), yet the $CD5^{+}$ B-1P population in the bone marrow likely to represent B-1a precursors was significantly reduced (Fig. 2c and Extended Fig. 2d). TrB-1a cells ($CD93^{+}IgM^{+}CD19^{+}B220^{lo}CD5^{+}$), known to exclusively generate B-1a cells [31] were also reduced to ~ 30% (Fig. 2d and Extended Fig.2e). In wild type mice, TrB-1a cells expressed high TCF1 and LEF1 compared with TrB cells (Extended Fig. 2f). TCF1 and LEF1 deficiency did not affect the earlier $Lin^{-}CD117^{hi}Sca\text{-}1^{+}$ (LSK) cells [33], hematopoietic stem cells (HSCs) and common lymphoid progenitor (CLP) cells (Extended Fig.2b). Taken together, TCF1 and LEF1 promote B-1a cell development from the earliest precursors.

TCF1 and LEF1 are required for B-1a cell self-renewal

TCF1 and LEF1 are important for proliferation and self-renewal of memory CD8+ T cells [34,35] and stem cells [35,36] . To gain insight into a possible role of TCF1/LEF1 in B-1a cell self-renewal, we first evaluated their proliferative state. TrB-1a cells have high expression of Ki-67 – a marker of proliferation, compared with TrB cells (Fig. 2e). Both the proliferative rate and expression of TCF1 and LEF1 were significantly higher in young (4–week-old) compared to adult (10–16-week-old) mice (Fig. 2f). In line with a failure to self-replenish in adult life, peritoneal B-1a cells lacking TCF1 and LEF1 failed to accumulate between 4 weeks to 14 weeks of age compared with the steady increase seen in littermate controls (Fig. 2g). To formally evaluate self-renewal, we adoptively transferred unmanipulated peritoneal cells from $TCF1^{WT}LEF1^{WT}$ or $TCF1^{\Delta}LEF1^{\Delta}$ ($CD45.2^{+}$) donors into wild-type ($CD45.1^{+}$) recipients, who received 5-bromodeoxyuridine (BrdU) in the drinking water for 12 days. Over 1% of wild-type B-1a cells had entered cell cycle, but this was reduced by over 90% in the absence of TCF1 and LEF1. Only a median of ~0.15% B-2 cells entered cell cycle over this period, and this did not change in the absence of TCF1/LEF1 (Fig. 2h). In a complementary approach that takes advantage of immunodeficient recipient mice that cannot repopulate the B-1a cell pool, we adoptively transferred 50:50 mixes of either CD45.2 $TCF1^{WT}LEF1^{WT}$: CD45.1 $TCF1^{WT}LEF1^{WT}$ or CD45.2 $TCF1^{\Delta}LEF1^{\Delta}$: CD45.1 $TCF1^{WT}LEF1^{WT}$ sorted peritoneal B-1a cells into unirradiated *Rag1*$^{-/-}$ mice. A smaller fraction of CD45.2 B-1a cells was found in both the peritoneal cavity and the spleen when donor B-1a cells lacked TCF1 and LEF1 (Extended Fig. 2g).

Since B-1a cell development and maintenance are also driven by BCR signalling [17], we asked whether TCF1 and LEF1 deficiency influenced BCR signalling and repertoire. Consistent with constitutive BCR signalling [37], phosphorylated Syk, Btk and BLNK could be readily detected ex vivo in B-1a cells in the absence of exogenous stimulation, but this was diminished in $TCF1^{\Delta}LEF1^{\Delta}$ B-1a cells (Extended Fig. 2h). scBCR-seq of peritoneal $CD19^{+}$ cells from adult mice revealed three B-1a-associated highly expanded clonal clusters with Ig V genes composed of heavy-chain and light-chain *Ighv11-2/ Igkv14-126* (c1), *Ighv12-3/Igkv4-91* (c2) and *Ighv9-3/ Iglv2* (c3) . These clusters were seen in both TCF1/LEF1 sufficient and deficient mice, with only a small reduction in c1and c2 and minor increase in c3 (Fig. 2i). Despite the decrease in total B-1a cells, the frequency of PtC-specific-cells remained unchanged in TCF1 and LEF1 sufficient vs deficient mice (Fig. 2j). High CD5 expression in peritoneal cavity B-1 cells is associated with clonal dominance [38]. In line with this, we observed loss of commonly restricted B-1 BCR repertoires - i.e. a more diverse BCR repertoire - in adult $TCF1^{\Delta}LEF1^{\Delta}$ peritoneal B cells (Fig. 2k) but not in neonatal immature B cells, which lack of B-1 specific clonotypes (data not shown). Thus, TCF1 and LEF1 enhance BCR signalling and CD5 expression, which are associated with the restricted BCR repertoire of B-1a cells.

We did not detect decreased serum antibodies of any isotype in mice lacking TCF1 and LEF1 (Extended Fig. 3a) suggesting that either a low number of B-1a cells is sufficient for production of natural antibody, or there is compensation by B-1 cell-derived plasma cells ($CD19^{lo}$ $CD138^{+}$ $IgM^{+}IgD^{-}CD43^{+}$) [39], which are unchanged in the spleens of TCF1/LEF1-deficient mice (Extended Fig. 3b). Although low in numbers, we also observed an increase in $IgG3^{+}$ B-1a cells in both peritoneal cavity and spleen (Fig. 3a) **and an increased** frequency of splenic B-1 pre-plasma cells ($CD19^{hi}CD138^{+}IgM^{+}IgD^{-}CD43^{+}$) [9,40] **in mice lacking** TCF1/LEF1 in B cells (Fig. 3b).

TCF1 and LEF1 promote B-1a cell mitosis and metabolism and limit differentiation.

We performed RNA sequencing (RNA-seq) analysis on purified $TCF1^{WT}LEF1^{WT}$ and $TCF1^{\Delta}LEF1^{\Delta}$ B-1a cells and expression of B-1a signature genes in these cells was superimposed onto the total genes shown to be differentially expressed between B-1a, B-1b cells and FO B cells from peritoneal cavity according to Immgen [41]. Overall, there was tight correlation in the transcriptional profiles of $TCF1^{WT}LEF1^{WT}$ and $TCF1^{\Delta}LEF1^{\Delta}$ B-1a cells suggesting that B-1a cell identity was largely maintained in the absence of TCF1/LEF1 (Fig. 3c). Amongst the differentially expressed genes, the B-1a signature gene *Cd5* was downregulated in $TCF1^{\Delta}LEF1^{\Delta}$ B-1a cells at both RNA and protein level (Fig.3d&e). $TCF1^{\Delta}LEF1^{\Delta}$ B-1a cells also expressed higher amounts of transcripts associated with B cell activation and plasma cell differentiation such as *Zbtb20* and *Satb1* [42–44] (Fig. 3d). Gene set enrichment analysis (GSEA) revealed that the top regulated pathways were linked to cell cycle including G2-M checkpoint (*Cdk1* and *Ccnb2*) and E2F targets (*E2f8* and *Cenpm*) (Fig. 3f and Extended Fig. 3c).

Importantly, the hallmark “Myc targets” pathway was downregulated, suggesting Myc may be a direct target of TCF1 and LEF1 in B-1a cells (Fig. 3g). In line with this, there was a strong and significant

correlation between the expression of Myc and the expression of both TCF1 and LEF1 (Fig. 3h). Myc is a master regulator of metabolism [45] and B-1 cells depend on glycolysis, acquisition of exogenous fatty acids and autophagy for self-renewal [46]. Consistent with this, inhibition of fatty acid metabolism, oxidative phosphorylation (OXPHO) and glycolysis pathways were also prominent hallmarks in the residual $TCF1^{\Delta}LEF1^{\Delta}$ B-1a cells (Fig. 3g). We also identified two additional transcriptional factors, *Ets1* and *Irf4*, downregulated in $TCF1^{\Delta}$, $LEF1^{\Delta}$, and $TCF1^{\Delta}LEF1^{\Delta}$ B-1a (Fig. 3i). Given previous a report showing B cell intrinsic roles of Ets1 on preventing non-cognate B cell activation and plasma cell differentiation [47], we investigated whether this transcription factor regulates B-1a cell numbers and found that B-1a cells were indeed reduced in the peritoneal cavity of mice lacking Ets1 in B cells (Fig. 3j).

Next, we looked into the targets of TCF1/LEF1 in B-1a cells. Due to low cell numbers and low-level expression of these transcription factors in B-1a cells, ChIP-seq in this population was not successful. Given the common overlap between transcription factor targets in B and T cells, we analysed TCF1 peaks from published ChIP-seq datasets of total mouse thymocytes [48] and compared these with open chromatin regions identified by ATAC-seq on B-1a cells from Vh12/Vk4 transgenic mice [27]. Notably, TCF1 peaks were found at the promoters or enhancers of *Cd5, Myc and Ets1* and these loci also harboured open chromatin regions in B-1a cells, suggesting they are direct targets of TCF1 in B-1a cells (Fig. 3k). Taken together, these results suggest that TCF1 and LEF1 are required for the self-renewal of B-1a through positively regulating cell cycle and metabolism, whilst negatively regulating terminal differentiation.

TCF1 and LEF1 promote IL-10 production by B-1a cells.

Next, we asked whether the absence of TCF1 and LEF1 in B-1a cells would affect their regulatory function. In mice, multiple subsets of IL-10-producing B cells have been described including B-1a cells ($CD19^{hi}B220^{lo}CD5^{hi}CD1d^{-}CD21^{-}CD23^{-}$) [5],B10 ($CD19^{+}B220^{+}CD5^{+}$ $CD1d^{hi}$ $CD21^{-}$ $CD23^{-}$) cells [10,49], marginal-zone (MZ) B cells ($CD19^{+}$ $B220^{+}IgM^{hi}IgD^{lo}CD21^{hi}CD23^{lo}CD5^{-}CD1d^{hi}$) [50] and $CD138^{+}$ plasma cells ($CD19^{lo}B220^{lo/-}$ $CD138^{+}$) [51]. Of all subsets, B-1a cells appear to transcribe the highest amounts of *Il10* mRNA (immgen.org probeSet ID: 10349603). Using the published 134 “B10-associated genes” and the related “Negative regulation of immune system” gene list [52] **we scored the expression of these genes in our scRNA-seq analysis of total peritoneal B cells**. Both of these gene signatures were upregulated in the B-1a cell clusters c1, c2 and c3 clusters (Fig. 2i and Fig. 4a, b), which also co-expressed *Tcf7*, *Cd5* and *Ctla4*. PD-L1, a molecule that curtails autoimmunity by limiting expansion and activity of effector T cells [53] was highly expressed in peritoneal B-1 cells compared to conventional B cells (Fig. 4c). Consistent with their regulatory and B10 features, the B-1 cells with highest TCF1/LEF1 expression produced 2-fold higher IL-10 upon activation compared to those expressing low amounts of TCF1/LEF1 (Fig. 4d). To investigate whether TCF1 and LEF1 regulate IL-10 production, we stimulated total peritoneal cells from $TCF1^{WT}LEF1^{WT}$ and $TCF1^{\Delta}LEF1^{\Delta}$ mice for 5 hours with LPS, PMA, ionomycin, and Brefeldin A. B-1a cells lacking TCF1 and LEF1 produced 50% less IL-10 compared to LEF1/TCF1 sufficient cells (Fig. 4e and

Extended Fig. 4a). Intravenous LPS injection induces Lag3^{+}CD138^{+} cells that are known to produce IL-10 [54]; these were decreased in mice lacking TCF1$^{\Delta}$LEF1$^{\Delta}$ in B cells (Extended Fig. 4b).

We were intrigued to find two subsets of splenic B cells producing different amounts of IL-10 according to the amount of CD19 expression in the presence or absence of stimulation. Whereas only CD19^{lo} cells produced IL-10 in the steady state, an increase in IL-10 production was only seen in the CD19^{hi} subset upon stimulation (Fig. 4f). While the CD19^{lo} subset exhibited the CD5^{+}CD1d^{+} phenotype characteristic of B10 cells [10], the CD19^{hi} subset displayed a B-1a phenotype, with higher CD5 and lower CD21, CD1d, and B220 expression (Fig. 4f). Consistent with splenic CD19^{hi} IL-10^{+} cells deriving from B-1a cells, they had the highest expression of TCF1 and LEF1 among IL-10 producing B cells (Fig. 4g and Extended Fig. 4c) and were significantly reduced in TCF1$^{\Delta}$LEF1$^{\Delta}$ mice (Fig. 4h). Together, our data revealed that TCF1 and LEF1 predominantly promote the generation of IL-10^{+} B-1a cells both from peritoneal cavity and spleen.

TCF1 and LEF1 promote anti-inflammatory properties of B-1a cells

B cells have been shown to play protective roles in human multiple sclerosis [55,56] and its EAE mouse model [57]. In the experimental model, such regulation requires B-1a cells rather than recirculating follicular B cells [58] and is dependent on IL-10 [57]. We therefore tested whether TCF1 and LEF1 were required for the regulatory function of B-1a in EAE. Activated peritoneal B-1 cells from TCF1^{WT}LEF1^{WT} and TCF1$^{\Delta}$LEF1$^{\Delta}$ mice were injected 3.5 days following immunization with myelin oligodendrocyte glycoprotein (MOG_{35-55}). Clinical disease severity was significantly reduced in mice receiving TCF1^{WT}LEF1^{WT} B-1 cells and onset was delayed compared to mice receiving TCF1$^{\Delta}$LEF1$^{\Delta}$ B-1 cells (Fig. 4i).

We next searched for autocrine roles of TCF1/LEF1-driven IL-10 in B-1 cells, since B-1 cell derived IL-10 represses proliferation [59,60]. TCF1 and LEF1 promoted plasma cell (PC) differentiation of B-1 cells cultured with LPS for 3 days and limited excessive proliferation of non-PCs (Fig. 5a-c). IL-10 blockade using IL-10R-Fc antibody partially mimicked the effect of TCF1/LE1 deficiency, suggesting that TCF1/LEF1 limits excessive proliferation at least in part through inducing IL-10 (Extended Fig. 4e).

TCF1/LEF1 are required for asymmetric cell division in CD8^{+} T cells so they can produce both effector Myc^{hi} cells and resting memory Myc^{lo} cells [61]. Much as seen in CD8^{+} T cells, Myc^{lo} B-1 cells appeared in the third division and these cells did not proliferate further (Fig. 5d). Such Myc^{lo} cells also downregulated CD19, CD86, FCRL5 and CD11b (Fig. 5d-f). By contrast, B-1a cells lacking TCF1 and LEF1 failed to generate Myc^{lo} cells, and continued to proliferate extensively (Fig. 5d), failing to downregulate CD19 and expressing even higher amounts of activation and exhaustion markers FCRL5 and CD86 (Fig. 5g). Such FCRL5^{+}CD86^{+}CD19^{hi} B cell phenotype has been described to characterise “exhausted” B cells [62] and is reminiscent of what are now known as “atypical memory B cells” or aged-associated B cells (ABCs) [63]. ABCs have been identified in patients with chronic infections in the context of HIV and common variable immunodeficiency [64,65], as well as in patients with autoimmune diseases [63]. Of note and as expected,

TCF1/LEF1 did not limit B-2 cell proliferation and Myc expression remained high as B-2 cells divided (Extended Fig. 4d and f). Strikingly, in the absence of TCF1/LEF1, PD-L1 was completely downregulated upon activation, independently of cell division (Fig. 5h). **ATAC-seq on B-1a cells** [27] revealed two chromatin accessible regions in the first two exons of *Cd274* (encoding PD-L1) (Fig. 5i), suggesting PD-L1 is a direct target of TCF1 and LEF1 as is the case in DP thymocytes [48]. Of note, expression of CD86, FCRL5 and PD-L1 in resting B-1 cells was comparable between $TCF1^{WT}LEF1^{WT}$ and $TCF1^{\Delta}LEF1^{\Delta}$ mice, indicating that TCF1/LEF1 are important to maintain PD-L1 expression and prevent CD86 and FCRL5 upregulation upon B-1 cell activation (Extended Fig. 4g). Together, these data suggest that TCF1/LEF1 enhances PD-L1 expression and IL-10 production, which prevents excessive cell proliferation and exhaustion to maintain their regulatory function.

Asymmetric cell division is a mechanism to generate stem-like CD8 T cells ($TCF1^{+}CD8^{+}$) with memory potential in situations of strong T cell stimulation [66]. Differences in Myc levels in daughter T cells regulate proliferation, metabolism, and differentiation [61]. Here we have shown that these principles also operate for B-1a cells but not for conventional B cells. It is tempting to speculate that TCF1 and LEF also control B-1a cell development and homeostasis via asymmetric cell division. The corollary is that B cell exhaustion and ABC formation may be an obligatory consequence of excessive proliferation in the absence of asymmetric cell division and/or in the absence of IL-10-mediated autoregulation. Further studies are required to investigate TCF1/LEF1-driven asymmetric cell division in B-1a cells and how dysregulation of this pathway may impact autoimmune, autoinflammatory, and infectious diseases as well as CLL, a B-1a-derived malignancy.

Methods And Materials

Mice. $Tcf7^{flox/flox}Lef1^{flox/flox}$ mice were generated by Hai-Hui Xue (Center for Discovery

& Innovation, US) [67,68]. $Mb1^{Cre}$ mice, $Rag1^{-/-}$ and CD45.1 mice were maintained on a C57BL/6 background and housed in specific pathogen free conditions at the Australian National University (ANU, Canberra, ACT, Australia) Bioscience Facility. $Tcf7^{flox/flox}Lef1^{flox/flox}$ mice were backcrossed at least 6 times onto the C57BL/6 background, then were subsequently crossed to $Mb1^{Cre}$ mice to generate conditional *Tcf1/Lef1*-knockout mice. Mice were used from 8-12 weeks, and they were age matched when comparing the effect of two genotypes, except for aging assessment (4-21 weeks). All mouse procedures were approved by the Australian National University's Animal Experimentation Ethics Committee or UK Home Office under project licence (PP2867252). $Ets1^{flox/flox}$ mice crossed more than 12 generations onto a C57BL/6 background were obtained from Dr Barbara Kee at the University of Chicago, US. CD19-Cre mice on a C57BL/6 background were obtained from Jackson Laboratories (Bar Harbor, ME, US) and crossed to $Ets1^{flox/flox}$ mice to generate knockout CD19-Cre $Ets1^{flox/flox}$ ($Ets1^{\Delta}$) [69] and control CD19-Cre ($Ets1^{WT}$) mice. Mice were used at both 9 weeks and 20 weeks of age to compare phenotypes. Mouse procedures involving Ets1 floxed mice were approved by the University at Buffalo IACUC.

Human Samples. Tonsillar tissue was obtained from consenting donors undergoing tonsillectomy at Calvary John James Hospital and The Canberra Hospital (Canberra, Australia) followed by being mechanically disrupted. The tonsillar lymphocyte and PBMCs were then purified by Ficoll Hypaque gradient centrifugation method (GE Healthcare Life Sciences). Experiments with human samples were approved the Human Experimentation Ethics Committee at The Australian National University and the University Hospital Institutional Review Board.

Flow Cytometry. Single-cell suspension from mouse peritoneal cavity, spleens and bone marrow were treated with TruStain FcX rat anti-mouse CD16/32 antibodies (BioLegend; cat # 101320). The cells were then stained with primary antibodies used for mouse samples along with LIVE/DEAD Fixable Aqua Dead Cell strain (Invitrogen), or ebioscience Fixable eFluor780 viability dye (Invitrogen). The primary antibodies included: B220-BUV737 (RA3-6B2, BD Horizon), CD19-BV605(6D5, Biolegend), CD23-BV421(B3B4, Biolegend), CD5-APC (53-7.3,ebioscience), IgM-PE-Cy7 (II/41,ebioscience), CD19-BUV395(1D3, BD Horizon), CD3-BV650 (17A2, Biolegend), CD21-BV605(7G6, Biolegend), IgD-PerCP/Cyanine5.5(11-26c.2a, Biolegend), CD93-BV480(AA4.1, Biolegend), CD24-Pacific Blue(M1/69, Biolegend), CD43-BV605(S7, Biolegend), CD3-APC-Cy7(17A2, Biolegend), CD4-APC-Cy7(GK1.5, Biolegend), CD11b-APC-Cy7(M1/70, Biolegend), TER119-APC-Cy7(TER-119, BD), Gr1-APC-Cy7(RB6-8C5, Biolegend), Sca-1-BV421(Ly-6A/E, Biolegend), c-Kit-APC(2B8, Biolegend), CD127-PE-Cy7(A7R34, Biolegend), CD16/32-PerCP/Cyanine5.5(93, Biolegend), CD135-PE(A2F10, Biolegend), CD45.1-BV711(A20, Biolegend), CD45.2-BUV737 (104, BD), CD274-BV711(B7-H1, Biolegend), CD86-PE-Cy7(GL-1, Biolegend), FCRL5-AF488(biotechne), c-Myc-AF647(Y69, abcam), TCF1/TCF7-AF488(C63D9, Cell Signaling Technology), LEF1-AF488(C12A5, Cell Signaling Technology), Rhodamine-DHPE Liposomes(DOPC/CHOL/Rhodamine-DHPE(54:45:1) were used (FormumMax, Sunnyvale,CA).

For cytokine intraceullular staining, the cells were stimulated with PMA, ionomycin and brefeldin A for the terminal 5h of culture. Cells were harvested and stained for surface markers, including ebioscience Fixable eFluor780 viability dye (Invitrogen) to exclude dead cells before cells were fixed. Intracellular staining was performed with Cytofix/Cytoperm kit (BD) with IL10-PE (JES5-16E3, Biolegend) as recommended. For transcription factors, eBioscience Foxp3/transcription factor staining buffer set (Invitrogen) was used per manufacturer's instructions.

Human tonsil cells and PBMC were treated with human TruStain FcX CD16/32/64 antibodies (Biolegend) and then stained with the following anti-human antibodies: CD3-BV785 (HIT3a, BD Bioscience), CD19-BUV737(SJ25C1, BD Bioscience), CD20-APC-Cy7(2H7, Biolegend), CD27-PE-Cy7(M-T271, BD Bioscience), CD38-FITC (HIT2, BD Bioscience), CD43-BV605(1G10, BD Horizon), TCF1/TCF7-AF488(C63D9, Cell Signaling Technology), LEF1-AF488(C12A5, Cell Signaling Technology). Flow cytometers (LSRFortessa X-20, FACSAria II and LSR II; BD) and software (CellQuest and FACSDiva; BD) were used for the acquisition of flow cytometric data, and FlowJo software (Tree Star, Inc.) was used for analysis.

Generation of bone-marrow and fetal-liver chimeras. To generate fetal-liver chimera, $1x10^6$ fetal liver cells from *Tcf7*$^{+/flox}$.*Lef1*$^{+/flox}$.Cre^{Mb1} or *Tcf7*$^{flox/flox}$.*Lef1*$^{flox/flox}$.Cre^{Mb1} mice (at embryonic day 14.5) were

transferred intravenously into sub-lethally irradiated (500 rad) *Rag1*$^{-/-}$ recipients. To generate bone marrow chimeras, 2 x 10^6 bone marrow- derived hematopoietic stem cells from 8 weeks old mice with aforementioned genotypes were transferred intravenously into sub-lethally irradiated *Rag1*$^{-/-}$ recipients. Mice were given Bactrim in their drinking water for 48 hr before injection and for 6 weeks after injection and housed in sterile cages. After 6 weeks of reconstitution, mice were taken down for phenotyping by flow cytometry.

Adoptive cell-transfer experiments. Equal numbers (1 x 10^5 cells) of flow-cytometry-sorted peritoneal CD19$^+$B220$^-$CD5$^+$CD23$^-$ B-1a cells from *Tcf7*$^{+/+}$.*Lef1*$^{+/+}$ (CD45.2$^+$) or *Tcf7*$^{flox/flox}$.*Lef1*$^{flox/flox}$.Cre^{Mb1} (CD45.2$^+$) and wild-type (CD45.1$^+$) were adoptively transferred into *Rag1*$^{-/-}$ recipients intraperitoneally, The frequency of donor B cells among total peritoneal B cells was analysed at 2 months after transfer.

Peritoneal cell transfer and In vivo BrdU incorporation assay. Peritoneal cells were harvested from *Tcf7*$^{+/+}$.*Lef1*$^{+/+}$ (CD45.2$^+$) or *Tcf7*$^{flox/flox}$.*Lef1*$^{flox/flox}$.Cre^{Mb1} (CD45.2$^+$) donors by injecting 5 ml of serum-free, DMEM medium without L-glutamine (Gibco) into the peritoneal cavity and withdraw as much fluid as possible, followed by centrifuging to harvest the cells; 3 x 10^6 cells were then injected intraperitoneally into the CD45.1 recipients. The recipients were fed with water containing 0.8 mg mL^{-1} BrdU for 12 days. Mice were then killed, spleen, and PerC cells were analysed by flow cytometry.

ELISA. Flat-bottom 96-well ELISA plates (#3855, Thermo Fisher) were coated with goat anti-mouse kappa-UNLB (#1050-01, Southern Biotech) overnight. The plates were subsequently washed and blocked using 1% bovine serum albumin (BSA) in 1x phosphate-buffered saline (PBS) for 1.5 hr at 37 °C. Serial dilution of the mouse serum was added to the wells and incubated overnight at 4C. Targeted antibodies were detected using AP-conjugated goat anti-mouse IgM (#1020-04, Southern Biotech) and AP-conjugated goat anti-mouse IgG3 (#1100-04, Southern Biotech). Plates were developed using 1 mg mL^{-1} phosphatase substrate tablets (#S0942, Sigma-Aldrich), and the absorbances at at 405 nm and 605 nm was measured using an Infinite® 200 PRO plate reader (Tecan) equipped with i-control™ version 1.9 software. Serum was added in serial dilution before addition of secondary antibody: AP-conjugated goat anti-mouse IgM (#1020-04, Southern Biotech) and AP-conjugated goat anti-mouse IgG3 (#1100-04, Southern Biotech).

Flow Cytometric Analysis of Intracellular IL-10 Synthesis

In brief, isolated leukocytes or purified cells were resuspended (1 x 10^6 cells mL^{-1}) with LPS (10 µg mL^{-1}), PMA, ionomycin, and Brefeldin A (1:500, Biolegend) for 5 hr. For IL-10 detection, cells were stained with surface markers followed by fixation, permeabilization with the Cytofix/Cytoperm kit (BD Bioscience) according to the manufacturer's instructions. For transcription factors, staining fixation was done using a transcription factor fixation/permeabilization kit (Invitrogen).

RNA-seq library preparation and data analysis. Total RNA was purified from sorted peritoneal B-1a cells ($CD19^+CD3^-B220^-CD5^+CD23^-7AAD^-$) using the PicoPure RNA isolation kit. Library construction and sequencing of were performed in the Biomolecular Resource Facility, the John Curtin School of Medical Research, ANU. The single end reads of 76bp sequencing was generated on a HiSeq2000 machine with a depth of more than 30 million reads per samples. The raw reads were aligned to the mm10 (GRCm38) genome assembly using hisat2 [70] and the mapped reads were assigned with FeatureCounts [v2.4] [71] based on genome-build GRCm38.p4 annotation and NCBI Refseq gene mode by removing ribosomal genes and non-coding RNA, respectively. Differential expression analyses were performed with voom-limma [72], after removal of lowly expressed genes and normalized using the trimmed mean of M-values method [73,74]. Significantly differentially expressed genes were identified by applying a Benjamini–Hochberg adjusted P value threshold of 0.05 [75]. Gene set enrichment or pathway analysis were performed using clusterProfiler [76] and Camera [77] against the gene ontology (GO) database, KEGG database and HALLMARK, C2 and C7 gene sets in the MSigDB (v7.5).

Single-Cell RNA sequencing. Peritoneal B cells ($CD19^+CD3^-7AAD^-$) from three 8 weeks old mice and immature B cells ($Lin^-CD19^+CD93^+IgM^+7AAD^-$) from spleen of four 9 days old mice were sorted by the FACS Aria II cell sorting system (BD Immunocytometry Systems, San Jose, CA, USA).10,000 cells per sample were run on the 10X Chromium platform (10XGenomics). Library preparation and sequencing were performed by the Australian Cancer Research Foundation Biomolecular Resource Facility, the John Curtin School of Medical Research, ANU according to the manufacturer's instructions for the Chromium Next GEM Single Cell 5'Kit v2. Two libraries were generated and measured mRNA transcript expression and BCR repertoire. The samples were sequenced using the NovaSeq 6000 (Illumina) system. The FASTQ files were aligned to the mm 10 mouse reference genome using 10XGenomics CellRanger pipeline v.6.0.1. Statistical analysis, clustering and visualization were conducted using Seurat v.4.0.1 in the R environment.

ChIP-seq analysis. FASTQ files were downloaded from NCBI's GEO database for TCF1 and LEF1 CHIP-seq data (SRP142342) [78]. FASTQ files were aligned to Enembl's mouse GRCm38 genome using BWA version 0.7.15. The resulting BAM files were sorted, duplicates marked and indexed using Picard version 2.1.1. Peaks were called using MAC2 version 2.1.1 that were enriched in TCF1 or LEF1 relative to input using default parameters. Peaks were annotated using homer version 4.8. BAM files were normalised to 10 million reads and IGVTools version 2.3.75 was used to generate coverage files.

ATAC-seq analysis. FASTQ files were downloaded from NCBI's GEO database for ATAC-seq samples in B-1a cells (GSM2461745) [27]. FASTQ files were aligned to Ensembl's mouse GRCm38 genome using BWA version 0.7.15. The resulting BAM files were sorted, duplicates marked and indexed using Picard version 2.1.1. IGVTools version 2.3.75 was used to generate coverage file for visualisation.

In vitro stimulation. Cells were cultured in RPMI 1640 medium supplemented with 10% FBS, 2 mM L-glutamine, 100 U penicillin-streptomycin, 0.1 mM non-essential amino acids, 100mM Hepes, and 55 μM 2-

mercaptoethanol at 37 °C in 5% CO_2. B-1 cells were magnetically purified from peritoneal cavity using Pan B cell isolation kit II (Miltenyi Biotec, 130-104-443) with anti-mouse CD45R (B220) antibody (Miltenyi Biotec, 130-110-707) and labelled with CellTrace™ Violet (Thermo Fisher, C34557) followed by stimulating with or without 5 μg ml^{-1} LPS (O111:B4, Sigma, L4391), 10 μg ml^{-1} InVivoMAb anti-mouse IL-10R (CD210) (BioXCell, BE0050) and its isotype control, InVivoMAb rat IgG1 isotype control, anti-horseradish peroxidase (BioXCell, BE0088) for 72 h.

EAE. EAE was induced by immunization with MOG_{35-55} peptide, emulsified in Complete Freund's adjuvant (Sigma-Aldrich) and pertussis toxin (Sigma-Aldrich). On Day 3.5 mice 2 x 10^5 B-1 cells that had been previously activated with R848 (0.1 μg mL^{-1}) for 48 hr were transferred intravenously. Mice were examined daily and scored using the following scoring system: 0-no disease, 1-loss of tail tonicity, 2- hind leg weakness, 3- complete hind leg paralysis, 3.5-complete hind leg paralysis with partial hind body paralysis, 4- full hind and foreleg paralysis, and 5- moribund or dead animals [79].

Statistical analyses. Statistical tests included student t test, Mann-Whitney (U test, two-tailed), Correlation, one-way ANOVA or two-way ANOVA using GraphPad Prism (GraphPad Software, USA). Linear regression model carried out with R project. Statistically significant differences are indicated as *, $P \leq 0.05$; **, $P \leq 0.01$; ***, $P \leq 0.001$; ****, $P \leq 0.0001$; and n.s., not significant.

Declarations

Acknowledgements: We thank Dinis Calado, Tony Chen and Anqi Xu for Myc staining method; the personnel of Science Technology Platforms (STPs) for assistance with FACS sorting and sequencing data analysis; Biological Research Facility (BRF) for animal care, The Francis Crick Institute, United Kingdom; the Australian Phenomics Facility (APF) for animal care; Harpreet Vohra and Mick Devoy from the CHASM facility (JCSMR) for assistance with FACS sorting; the personnel of the Australian Cancer Research Foundation Biomolecular Resource Facility (JCSMR) for Sanger sequencing. This work was funded by NHMRC grants to CGV, Crick CC2228 grant to CGV.

Author contributions: Conceptualization: Q.S., C.G.V.; Methodology: Q.S.; Formal analysis: Q.S., H.W., J.A.R.; Investigation: Q.S., H.W., X.M., P.F.C., P.G.F., Y.Z., L.A.G.; Resources: H.-H.X, L.A.G.; Data Curation: J.A.R, Z.-P.F., P.C.; Writing - Original Draft: Q.S., C.G.V.; Writing - Review & Editing: Q.S., C.G.V.; Visualization: Q.S., H.W., X.M., J.A.R., Z.-P.F., P.C.; Supervision: Q.S., C.G.V.; Project administration: Q.S., C.G.V; Funding acquisition: C.G.V.

Competing interests: Authors declare no competing interests.

Data and materials availability: Bulk RNA-seq and scRNA-seq data relating to the Fig. 1, Fig.2, Fig3 and Fig. 4 have been deposited in (*to be provided*); with accession number (*to be provided*).

Code availability: N/A

References

1. Baumgarth, N. The double life of a B-1 cell: self-reactivity selects for protective effector functions. *Nat Rev Immunol* **11**, 34–46 (2011).
2. Berland, R. & Wortis, H. H. Origins and Functions of B-1 Cells with Notes on the Role of CD5. *Annu Rev Immunol* **20**, 253–300 (2003).
3. Smith, F. L. & Baumgarth, N. B-1 cell responses to infections. *Curr Opin Immunol* **57**, 23–31 (2019).
4. Suzuki, K., Maruya, M., Kawamoto, S. & Fagarasan, S. Roles of B-1 and B-2 cells in innate and acquired IgA-mediated immunity. *Immunol Rev* **237**, 180–190 (2010).
5. O'garra, A. *et al.* Ly-1 B (B-1) cells are the main source of B cell-derived interleukin 10. *Eur J Immunol* **22**, 711–717 (1992).
6. Heng, T. S. P. *et al.* The Immunological Genome Project: networks of gene expression in immune cells. *Nat Immunol* **9**, 1091–1094 (2008).- see Il10 probeSet ID:10349603 in B cells.
7. Saraiva, M. & O'Garra, A. The regulation of IL-10 production by immune cells. *Nat Rev Immunol* **10**, 170–181 (2010).
8. Hardy, R. R. B-1 B Cell Development. *The Journal of Immunology* **177**, 2749–2754 (2006).
9. Yang, Y., Tung, J. W., Ghosn, E. E. B., Herzenberg, L. A. & Herzenberg, L. A. Division and differentiation of natural antibody-producing cells in mouse spleen. *Proc Natl Acad Sci U S A* **104**, 4542–4546 (2007).
10. Yanaba, K. *et al.* A Regulatory B Cell Subset with a Unique CD1dhiCD5+ Phenotype Controls T Cell-Dependent Inflammatory Responses. *Immunity* **28**, 639–650 (2008).
11. Matsushita, T. *et al.* Inhibitory Role of CD19 in the Progression of Experimental Autoimmune Encephalomyelitis by Regulating Cytokine Response. *Am J Pathol* **168**, 812–821 (2006).
12. Aziz, M., Holodick, N. E., Rothstein, T. L. & Wang, P. The role of B-1 cells in inflammation. *Immunologic Research 2015 63:1* **63**, 153–166 (2015).
13. Mauri, C. Novel Frontiers in Regulatory B cells. *Immunol Rev* **299**, 5–9 (2021).
14. Dilillo, D. J. *et al.* Chronic lymphocytic leukemia and regulatory B cells share IL-10 competence and immunosuppressive function. *Leukemia* **27**, 170–182 (2012).
15. Saulep-Easton, D. *et al.* The BAFF receptor TACI controls IL-10 production by regulatory B cells and CLL B cells. *Leukemia* **30**, 163–172 (2015).
16. Yang, Y. *et al.* Distinct mechanisms define murine B cell lineage immunoglobulin heavy chain (IgH) repertoires. *Elife* **4**, (2015).
17. Graf, R. *et al.* BCR-dependent lineage plasticity in mature B cells. *Science (1979)* **363**, 748–753 (2019).
18. Hao, Z. & Rajewsky, K. Homeostasis of Peripheral B Cells in the Absence of B Cell Influx from the Bone Marrow. *Journal of Experimental Medicine* **194**, 1151–1164 (2001).

19. Martin, F. & Kearney, J. F. B-cell subsets and the mature preimmune repertoire. Marginal zone and B1 B cells as part of a “natural immune memory”. *Immunol Rev* **175**, 70–79 (2000).
20. Hayakawa, K., Hardy, R. R., Stall, A. M., Herzenberg, L. A. & Herzenberg, L. A. Immunoglobulin-bearing B cells reconstitute and maintain the murine Ly-1 B cell lineage. *Eur J Immunol* **16**, 1313–1316 (1986).
21. Kantor, A. B., Stall, A. M., Adams, S., Herzenberg, L. A. & Herzenberg, L. A. Differential development of progenitor activity for three B-cell lineages. *Proceedings of the National Academy of Sciences* **89**, 3320–3324 (1992).
22. Förster, I., Vieira, P. & Rajewsky, K. Flow cytometric analysis of cell proliferation dynamics in the B cell compartment of the mouse. *Int Immunol* **1**, 321–331 (1989).
23. Deenen, G. J. & Kroese, F. G. M. Kinetics of peritoneal B-1a cells (CD5 B cells) in young adult mice. *Eur J Immunol* **23**, 12–16 (1993).
24. Baumgarth, N. A Hard(y) Look at B-1 Cell Development and Function. *The Journal of Immunology* **199**, 3387–3394 (2017).
25. Johnson, J. L. *et al.* Lineage-Determining Transcription Factor TCF-1 Initiates the Epigenetic Identity of T Cells. *Immunity* **48**, 243-257.e10 (2018).
26. Kratchmarov, R., Magun, A. M. & Reiner, S. L. TCF1 expression marks self-renewing human CD8+ T cells. *Blood Adv* **2**, 1685–1690 (2018).
27. Kreslavsky, T. *et al.* Essential role for the transcription factor Bhlhe41 in regulating the development, self-renewal and BCR repertoire of B-1a cells. *Nat Immunol* **18**, 442–455 (2017).
28. Xing, S. *et al.* Tcf1 and Lef1 transcription factors establish CD8+ T cell identity through intrinsic HDAC activity. *Nat Immunol* **17**, 695–703 (2016).
29. Zhao, X., Zhu, S., Peng, W. & Xue, H.-H. The Interplay of Transcription and Genome Topology Programs T Cell Development and Differentiation. *The Journal of Immunology* **209**, 2269–2278 (2022).
30. Hobeika, E. *et al.* Testing gene function early in the B cell lineage in mb1-cre mice. *Proc Natl Acad Sci U S A* **103**, 13789–13794 (2006).
31. Pedersen, G. K. *et al.* B-1a transitional cells are phenotypically distinct and are lacking in mice deficient in IκBNS. *Proc Natl Acad Sci U S A* **111**, E4119–E4126 (2014).
32. Montecino-Rodriguez, E. & Dorshkind, K. B-1 B Cell Development in the Fetus and Adult. *Immunity* **36**, 13–21 (2012).
33. Yu, S. *et al.* Hematopoietic and leukemic stem cells have distinct dependence on Tcf1 and Lef1 transcription factors. *Journal of Biological Chemistry* **291**, 11148–11160 (2016).
34. Wu, J. Q. *et al.* Tcf7 Is an Important Regulator of the Switch of Self-Renewal and Differentiation in a Multipotential Hematopoietic Cell Line. *PLoS Genet* **8**, e1002565 (2012).
35. Moreira, S. *et al.* A Single TCF Transcription Factor, Regardless of Its Activation Capacity, Is Sufficient for Effective Trilineage Differentiation of ESCs. *Cell Rep* **20**, 2424–2438 (2017).

36. Read, R., St. Cyr, J., Marek, J., Whitman, G. & Hopeman, A. Bronchial anomaly of the right upper lobe. *Ann Thorac Surg* **50**, 980–981 (1990).
37. Wong, S. C. *et al.* Peritoneal CD5+ B-1 cells have signaling properties similar to tolerant B cells. *Journal of Biological Chemistry* **277**, 30707–30715 (2002).
38. Vanhee, S. *et al.* Lin28b controls a neonatal to adult switch in B cell positive selection. *Sci Immunol* **4**, (2019).
39. Smith, F. L. *et al.* B-1 plasma cells require non-cognate CD4 T cell help to generate a unique repertoire of natural IgM. *Journal of Experimental Medicine* **220**, (2023).
40. Savage, H. P. *et al.* Blimp-1–dependent and –independent natural antibody production by B-1 and B-1–derived plasma cells. *Journal of Experimental Medicine* **214**, 2777–2794 (2017).
41. Sun, J. *et al.* Transcriptomics Identify CD9 as a Marker of Murine IL-10-Competent Regulatory B Cells. *Cell Rep* **13**, 1110–1117 (2015).
42. Kitagawa, Y. *et al.* Guidance of regulatory T cell development by Satb1-dependent super-enhancer establishment. *Nat Immunol* **18**, 173–183 (2016).
43. Liu, J. *et al.* Deceleration of glycometabolism impedes IgG-producing B-cell-mediated tumor elimination by targeting SATB1. *Immunology* **156**, 56–68 (2019).
44. Chevrier, S. *et al.* The BTB-ZF transcription factor Zbtb20 is driven by Irf4 to promote plasma cell differentiation and longevity. *Journal of Experimental Medicine* **211**, 827–840 (2014).
45. Hao, Y. H. *et al.* Induction of LEF1 by MYC activates the WNT pathway and maintains cell proliferation. *Cell Communication and Signaling* **17**, 1–16 (2019).
46. Clarke, A. J., Riffelmacher, T., Braas, D., Cornall, R. J. & Simon, A. K. B1a B cells require autophagy for metabolic homeostasis and self-renewal. *Journal of Experimental Medicine* **215**, 399–413 (2018).
47. Russell, L. *et al.* Requirement for Transcription Factor Ets1 in B Cell Tolerance to Self-Antigens. *The Journal of Immunology* **195**, 3574–3583 (2015).
48. Emmanuel, A. O. *et al.* TCF-1 and HEB cooperate to establish the epigenetic and transcription profiles of CD4+CD8+ thymocytes. *Nature Immunology 2018 19:12* **19**, 1366–1378 (2018).
49. Yoshizaki, A. *et al.* Regulatory B cells control T-cell autoimmunity through IL-21-dependent cognate interactions. *Nature 2012 491:7423* **491**, 264–268 (2012).
50. Gray, M., Miles, K., Salter, D., Gray, D. & Savill, J. Apoptotic cells protect mice from autoimmune inflammation by the induction of regulatory B cells. *Proc Natl Acad Sci U S A* **104**, 14080–14085 (2007).
51. Neves, P. *et al.* Signaling via the MyD88 Adaptor Protein in B Cells Suppresses Protective Immunity during Salmonella typhimurium Infection. *Immunity* **33**, 777–790 (2010).
52. Yang, S. Y. *et al.* Characterization of Organ-Specific Regulatory B Cells Using Single-Cell RNA Sequencing. *Front Immunol* **12**, 711980 (2021).
53. Khan, A. R. *et al.* PD-L1hi B cells are critical regulators of humoral immunity. *Nat Commun* **6**, 1–16 (2015).

54. Lino, A. C. *et al.* LAG-3 Inhibitory Receptor Expression Identifies Immunosuppressive Natural Regulatory Plasma Cells. *Immunity* **49**, 120-133.e9 (2018).
55. Benedetti, L. *et al.* Relapses After Treatment With Rituximab in a Patient With Multiple Sclerosis and Anti–Myelin-Associated Glycoprotein Polyneuropathy. *Arch Neurol* **64**, 1531–1533 (2007).
56. Duddy, M. *et al.* Distinct Effector Cytokine Profiles of Memory and Naive Human B Cell Subsets and Implication in Multiple Sclerosis. *The Journal of Immunology* **178**, 6092–6099 (2007).
57. Fillatreau, S., Sweenie, C. H., McGeachy, M. J., Gray, D. & Anderton, S. M. B cells regulate autoimmunity by provision of IL-10. *Nat Immunol* **3**, 944–950 (2002).
58. Miles, K. *et al.* Immune tolerance to apoptotic self is mediated primarily by regulatory B1a cells. *Front Immunol* **8**, 298424 (2018).
59. Heine, G. *et al.* Autocrine IL-10 promotes human B-cell differentiation into IgM- or IgG-secreting plasmablasts. *Eur J Immunol* **44**, 1615–1621 (2014).
60. Sindhava, V., Woodman, M. E., Stevenson, B. & Bondada, S. Interleukin-10 Mediated Autoregulation of Murine B-1 B-Cells and Its Role in Borrelia hermsii Infection. *PLoS One* **5**, e11445 (2010).
61. Verbist, K. C. *et al.* Metabolic maintenance of cell asymmetry following division in activated T lymphocytes. *Nature* **532**, 389–393 (2016).
62. Roe, K. NK-cell exhaustion, B-cell exhaustion and T-cell exhaustion—the differences and similarities. *Immunology* **166**, 155–168 (2022).
63. Cancro, M. P. Age-Associated B Cells. *Annu Rev Immunol* **38**, 315–340 (2020).
64. Rakhmanov, M. *et al.* Circulating CD21low B cells in common variable immunodeficiency resemble tissue homing, innate-like B cells. *Proc Natl Acad Sci U S A* **106**, 13451–13456 (2009).
65. Moir, S. *et al.* Evidence for HIV-associated B cell exhaustion in a dysfunctional memory B cell compartment in HIV-infected viremic individuals. *Journal of Experimental Medicine* **205**, 1797–1805 (2008).
66. Gräbnitz, F. *et al.* Asymmetric cell division safeguards memory CD8 T cell development. *Cell Rep* **42**, (2023).
67. Steinke, F. C. *et al.* TCF-1 and LEF-1 act upstream of Th-POK to promote CD4+ T cell lineage choice and cooperate with Runx3 to silence the Cd4 gene in CD8+ T cells. *Nat Immunol* **15**, 646 (2014).
68. Yu, S. *et al.* The TCF-1 and LEF-1 Transcription Factors Have Cooperative and Opposing Roles in T Cell Development and Malignancy. *Immunity* **37**, 813–826 (2012).
69. Zook, E. C. *et al.* The ETS1 transcription factor is required for the development and cytokine-induced expansion of ILC2. *Journal of Experimental Medicine* **213**, 687–696 (2016).
70. Kim, D., Paggi, J. M., Park, C., Bennett, C. & Salzberg, S. L. Graph-based genome alignment and genotyping with HISAT2 and HISAT-genotype. *Nat Biotechnol* **37**, 907–915 (2019).
71. Liao, Y., Smyth, G. K. & Shi, W. featureCounts: an efficient general purpose program for assigning sequence reads to genomic features. *Bioinformatics* **30**, 923–930 (2014).

72. Ritchie, M. E. *et al.* limma powers differential expression analyses for RNA-sequencing and microarray studies. *Nucleic Acids Res* **43**, e47–e47 (2015).
73. Bourgon, R., Gentleman, R. & Huber, W. Independent filtering increases detection power for high-throughput experiments. *Proc Natl Acad Sci U S A* **107**, 9546–9551 (2010).
74. Robinson, M. D. & Oshlack, A. A scaling normalization method for differential expression analysis of RNA-seq data. *Genome Biol* **11**, 1–9 (2010).
75. Benjamini, Y. & Hochberg, Y. Controlling the False Discovery Rate: A Practical and Powerful Approach to Multiple Testing. *Journal of the Royal Statistical Society: Series B (Methodological)* **57**, 289–300 (1995).
76. Yu, G., Wang, L. G., Han, Y. & He, Q. Y. clusterProfiler: an R package for comparing biological themes among gene clusters. *OMICS* **16**, 284–287 (2012).
77. Wu, D. & Smyth, G. K. Camera: a competitive gene set test accounting for inter-gene correlation. *Nucleic Acids Res* **40**, e133–e133 (2012).
78. Emmanuel, A. O. *et al.* TCF-1 and HEB cooperate to establish the epigenetic and transcription profiles of CD4+CD8+ thymocytes. *Nat Immunol* **19**, 1366–1378 (2018).
79. Wang, R. X. *et al.* Interleukin-35 induces regulatory B cells that suppress autoimmune disease. *Nat Med* **20**, 633–641 (2014).
80. Chao, A. *et al.* Rarefaction and extrapolation with Hill numbers: a framework for sampling and estimation in species diversity studies. *Ecol Monogr* **84**, 45–67 (2014).

Figures

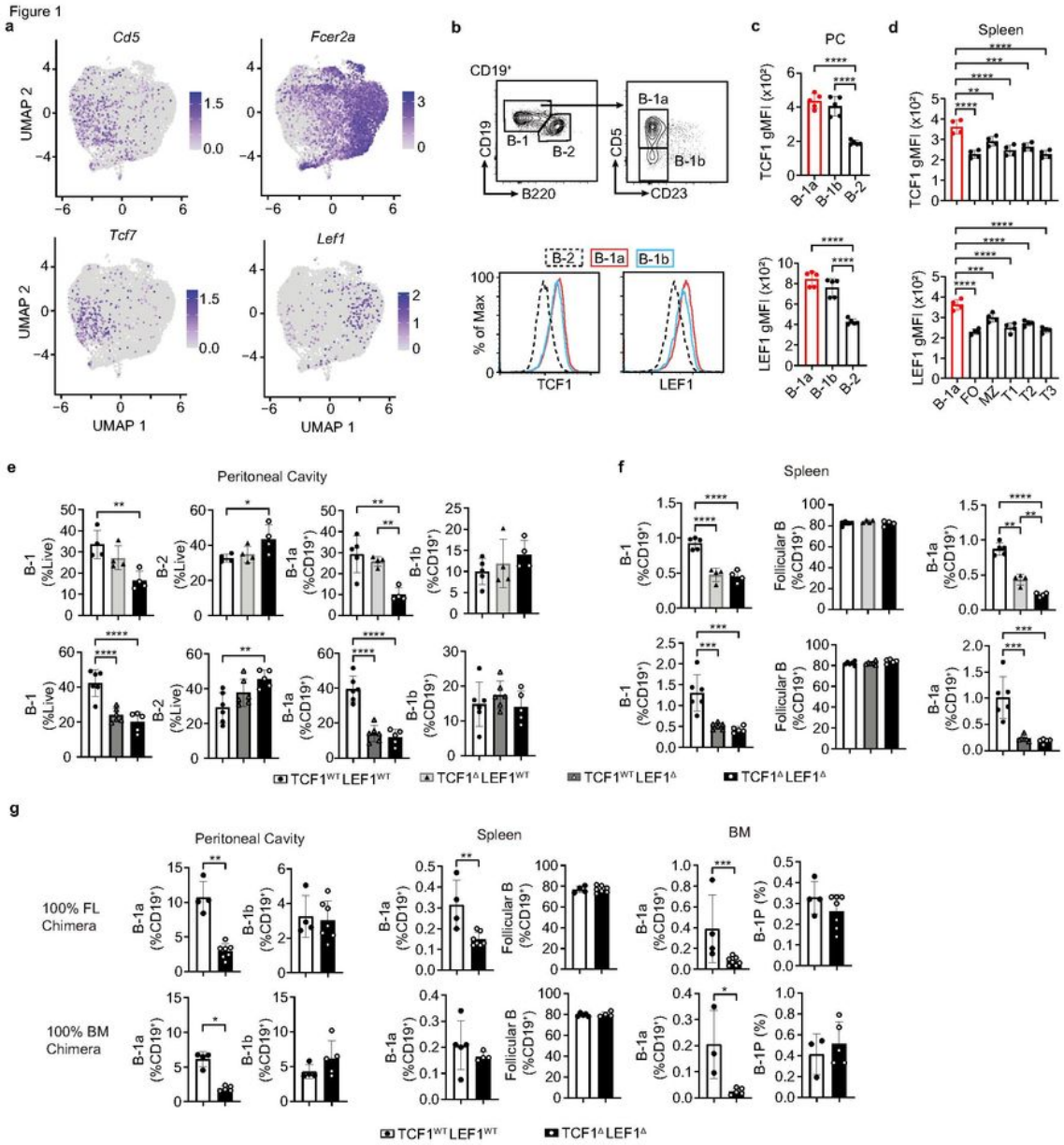

Figure 1

TCF1 and LEF1 expression and TCF1/LEF1 deficient mice phenotype. (a) Gene expression in the different clusters projected on UMAP of scRNA-seq on total peritoneal B cells. Color scaled for each gene with log-normalized gene expression level noted. (b-d) Flow cytometry gating strategy of peritoneal B-1a, B-1b and B-2 (upper), histogram of TCF1 and LEF1 expression (bottom) (b) and geometric mean fluorescence intensity (gMFI) quantification of TCF1 and LEF1 in B cells subsets from peritoneal cavity (c), and FO

(follicular B), MZ (marginal zone B), T1 (transitional 1), T2 (transitional 2), T3 (transitional 3) from spleen of C57BL/6J mice (d). (e-f) Quantification of the percentage of B-1 cells ($CD19^+B220^{lo/-}CD3^-$), B-2 cells ($CD19^+B220^+CD3^-$), B-1a cells ($CD19^+B220^{lo/-}CD5^+CD23^-$) and B-1b cells ($CD19^+B220^{lo/-}CD5^-CD23^-$), Follicular B cells ($CD19^+B220^+CD23^+CD21^-$) of peritoneal cavity (e) and spleen(f) from $TCF1^{WT}LEF1^{WT}$, $TCF1^{\Delta}$, $LEF1^{\Delta}$, $TCF1^{\Delta}LEF1^{\Delta}$ mice. (g) Frequency of various peritoneal, splenic and bone marrow (BM) B cell populations from sub-lethally irradiated $Rag1^{-/-}$ recipient mice 6 weeks after transferring fetal liver cells (at embryo day 14.5) or bone marrow (8-10 weeks old) from $TCF1^{WT}LEF1^{WT}$ and $TCF1^{\Delta}LEF1^{\Delta}$ mice. Each symbol represents an individual mouse, Data are mean ± s.d. Data are from one experiment representative of two independent experiment with a total of five mice (b-d), one experiment with five or seven mice per genotype, representative of three independent experiments (e-f), one experiment representative of four independent experiments with 4-10 chimeric mice(g). Statistical analysis was performed using parametric t test (b-d), Mann-Whitney t test (c-f). *$P < 0.05$, **$P < 0.001$ and ***$P < 0.0001$.

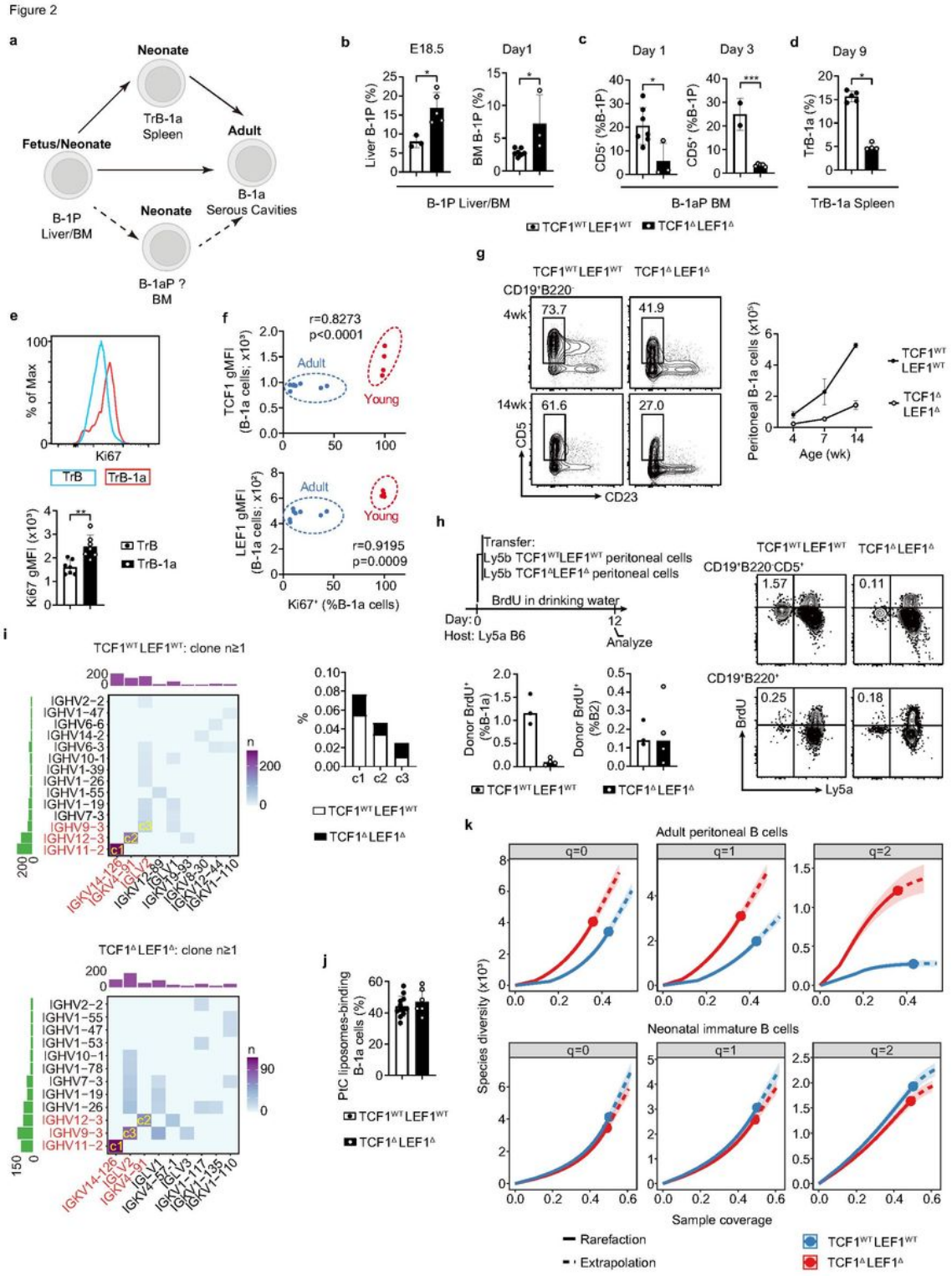

Figure 2

Regulation of B-1a cell development by TCF1 and LEF1. (a) A diagram of key stages of B-1a development. (b-d) Quantification of the frequency of $CD19^{+}B220^{-}Lin^{-}IgM^{-}CD93^{+}$ B-1 progenitors (B-1P) from $TCF1^{WT}LEF1^{WT}$ and $TCF1^{\Delta}LEF1^{\Delta}$ fetal liver (at embryo day 18.5), and bone marrow (BM) at postnatal day 1 (b), B-1aP ($CD19^{+}B220^{-}Lin^{-}IgM^{-}CD93^{+}$ $CD5^{+}$) from bone marrow at postnatal day 1 and 3

of $TCF1^{WT}LEF1^{WT}$ and $TCF1^{\Delta}LEF1^{\Delta}$ mice (c) and transitional B-1a cells (TrB-1a), identified as $CD93^{+}IgM^{+}CD19^{+}B220^{lo}CD5^{+}$ from spleen of neonatal $TCF1^{WT}LEF1^{WT}$ and $TCF1^{\Delta}LEF1^{\Delta}$ mice (postnatal day 9) (d). (e) Flow cytometry plot and quantification of gMFI of Ki67 in TrB-1a and TrB cells of $TCF1^{WT}LEF1^{WT}$ at day 9. (f) Correlation analysis between expression of TCF1 or LEF1 and percentage of Ki67 positive cells in B-1a cells. 4 weeks old mice (Young, n=4) and 8-16 weeks old mice (Adult, n=8). (g) Flow cytometry plots of B-1a cells from $TCF1^{WT}LEF1^{WT}$ and $TCF1^{\Delta}LEF1^{\Delta}$ mice at 4 weeks of age (top) and 14 weeks of age (bottom), gated on peritoneal $CD19^{+}B220^{-}$ cells (left), quantification of total B-1a cell as at left (right). (h) Treatment protocol of BrdU labelling to donor $TCF1^{WT}LEF1^{WT}$ and $TCF1^{\Delta}LEF1^{\Delta}$ B cells (ly5b) in wild-type (ly5a) recipient mice for 12 days after intraperitoneal injection of equal number (2×10^{6}) peritoneal cells (top left), flow cytometry plots (right) and quantification of percentage of BrdU labelled cells in donor B-1a or B-2 cells (bottom left). (i)Heatmap and quantification of the frequency of clones with a particular V_H-V_L pairing from $TCF1^{WT}LEF1^{WT}$ and $TCF1^{\Delta}LEF1^{\Delta}$ peritoneal B cells. Heatmap shows the number of clones. Row and column histograms indicate V_H and V_L number, respectively. The clones with *Ighv11-2/Igkv14-126*, *Ighv12-3/Igkv4-91* and *Ighv9-3/Iglv2* were labelled as c1, c2, c3 respectively (left) and quantification of frequency of clones of c1, c2 and c3 (right). (j) Frequency of liposome-binding B-1a cells in $TCF1^{WT}LEF1^{WT}$ and $TCF1^{\Delta}LEF1^{\Delta}$ mice. (k) Coverage-based diversity accumulation curve for Hill numbers of order (q=0, 1 and 2), i.e., species richness, Shannon entropy and Simpson index, respectively . Each symbol represents an individual mouse, Data are mean ± s.d and median (h). Data are from one experiment representative of two independent experiment with three or eight mice per genotype (b-d), Data are from two independent experiment with a total of five or ten mice per genotype (e), one experiment with three or five mice per genotype, representative of two independent experiments (f-h), Data are from two independent experiments with a total of eight or twelve mice per genotype (j). Statistical analysis was performed using Mann-Whitney t test (a-e, h). *$P < 0.05$, **$P < 0.001$ and ***$P < 0.0001$.

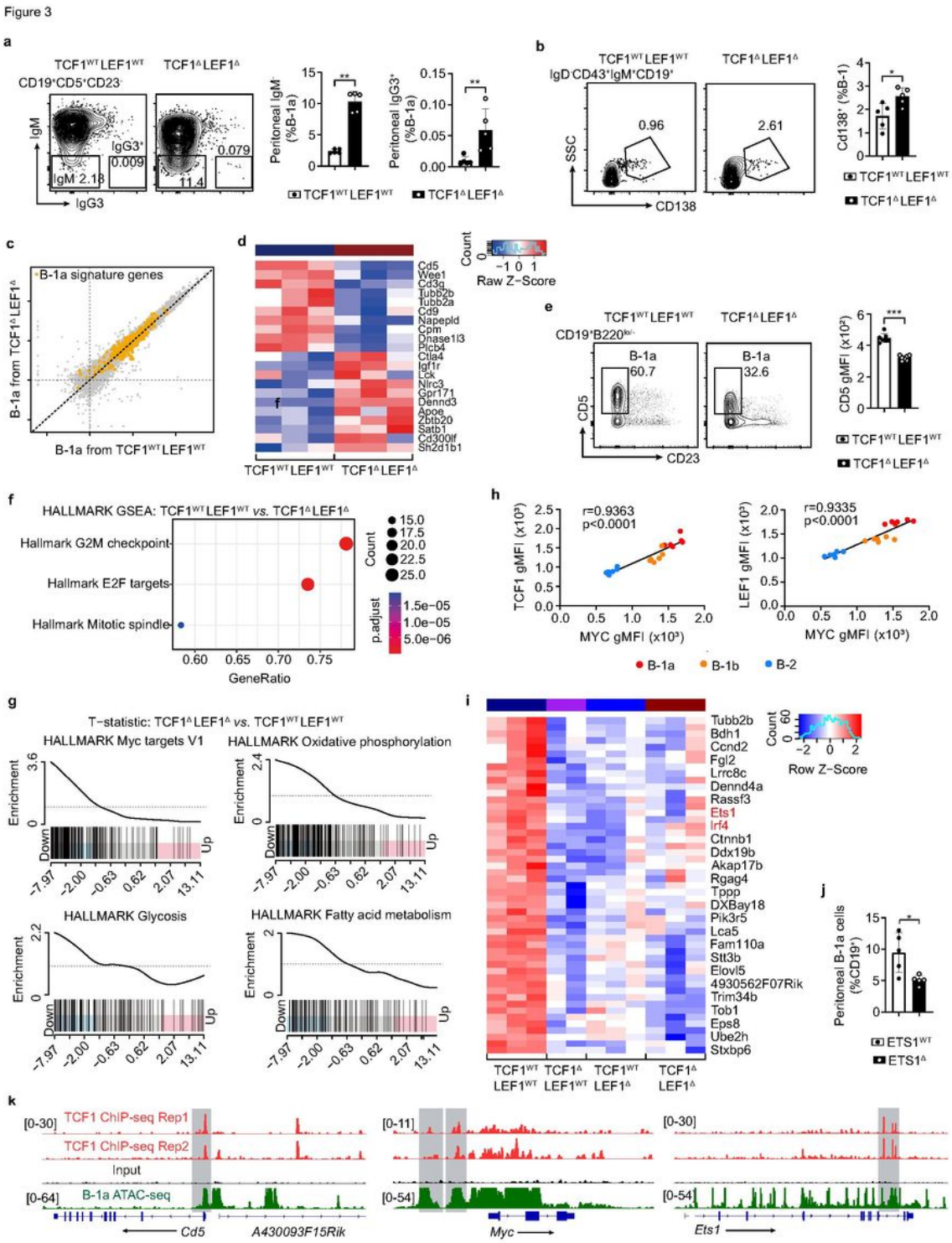

Figure 3

TCF1 and LEF1 promote B-1a cell mitosis and metabolism and limit differentiation.

(a) Flow cytometry plots (left) and quantification of percentage (right) of IgM^- or $IgG3^+$ from peritoneal B-1a cells in $TCF1^{WT}LEF1^{WT}$ and $TCF1^{\Delta}LEF1^{\Delta}$ mice. (b) Flow cytometry plots (left) and quantification of percentage (right) of $CD138^+$ cells from $TCF1^{WT}LEF1^{WT}$ and $TCF1^{\Delta}LEF1^{\Delta}$ B-1 cells. (c) Expression-

expression plot of transcriptomes of B-1a cells isolated from $TCF1^{WT}LEF1^{WT}$ and $TCF1^{\Delta}LEF1^{\Delta}$ mice. Superimposed B-1a signature genes from published RNA-seq data which over- or under-represented in peritoneal B-1a versus B-1b cells . (d) Expression heatmap of B-1a signature genes, with the color representing normalized RPM for each gene across different samples. (e) Flow cytometry plots (left) and quantification of CD5 gMFI (right) from $TCF1^{WT}LEF1^{WT}$ and $TCF1^{\Delta}LEF1^{\Delta}$ B-1a cells. (f) Dot plot presentation of Hallmark gene sets upon a GSEA for differentially expressed genes in $TCF1^{WT}LEF1^{WT}$ and $TCF1^{\Delta}LEF1^{\Delta}$ B-1a cells. (g) GSEA on RNA-seq data shows enrichment for Myc signalling (top left), Oxidative phosphorylation signalling (top right), Glycolysis signalling (bottom left), fatty acid metabolism signalling (bottom right) from $TCF1^{WT}LEF1^{WT}$ and $TCF1^{\Delta}LEF1^{\Delta}$ B-1a cells. (h) Correlation analysis between expression of TCF1 or LEF1 and expression of Myc in peritoneal B-1a, B-1b and B-2 cells. (i) Expression heatmap of B-1a signature genes, with the color representing normalized RPM for each gene from B-1a cells of $TCF1^{WT}LEF1^{WT}$, $TCF1^{\Delta}$, $LEF1^{\Delta}$ and $TCF1^{\Delta}LEF1^{\Delta}$ mice. (j) Quantification of percentage (right) of peritoneal B-1a cells from $Ets1^{WT}$ (*Ets1*$^{+/+}$.Cre^{Cd19}) and $Ets1^{\Delta}$ (*Ets1*$^{flox/flox}$.Cre^{Cd19}) mice. (k) ChIP-seq analysis of TCF1 and LEF1 binding in $CD4^{+}CD8^{+}$ thymocytes and ATAC-seq analysis at *Cd5*, *Myc* and *Ets1* on B-1a cells from *Vh12/Vk4* transgenic mice . Each symbol represents an individual mouse, Data are mean ± s.d. One experiment with five mice per genotype, representative of two or three independent experiments (a-b, e), Statistical analysis was performed using Mann-Whitney t test (b, d-e). *P < 0.05, **P < 0.001 and ***P < 0.0001.

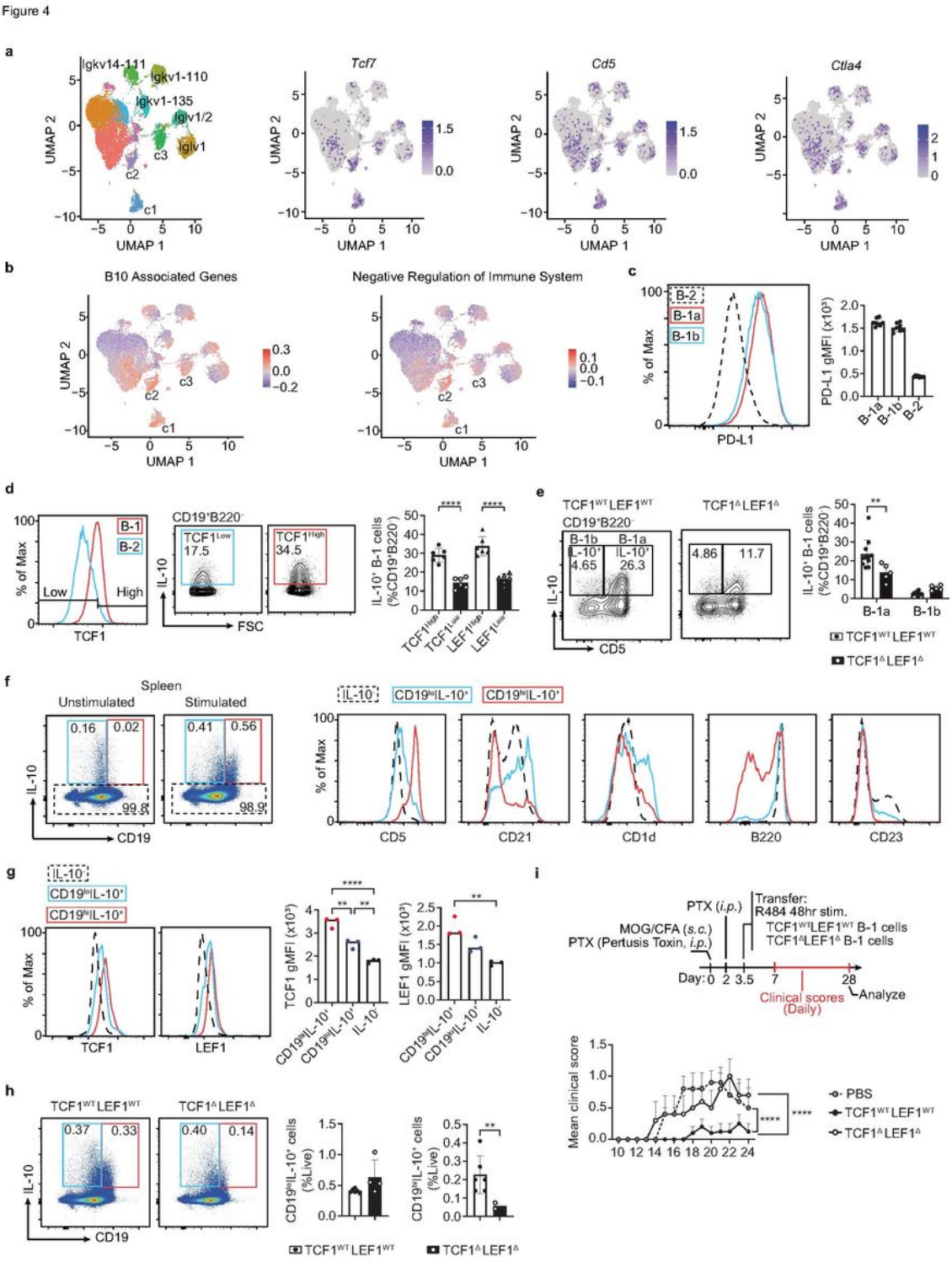

Figure 4

TCF1 and LEF1 regulate IL-10 production on B-1a cells. (a) UMAP plots showing the BCR clusters of peritoneal B cells and expression of *Tcf7*, *Cd5* and *Ctla4* in different clusters. Color scaled for each gene with log-normalized gene expression level noted. (b) Evaluation of the B10 signatures and negative regulation of immune system associated genes module score. (c) Flow cytometry plots (left) and quantification of percentage (right) of IL-10^{+} cells in TCF1^{High} or TCF1^{Low} B-1 cells from peritoneal cavity.

Lymphocytes were cultured with LPS, PMA, ionomycin and brefeldin A for 5 hr before staining. (d) Flow cytometry plots (left) and quantification of percentage (right) of IL-10^{+} cells in B-1 cells from TCF1^{WT}LEF1^{WT} and TCF1$^{\Delta}$LEF1$^{\Delta}$ peritoneal cells. Cells were cultured with LPS, PMA, ionomycin and brefeldin A for 5 hr before staining. (e) Cell surface makers expression by CD19^{lo}IL-10^{+} (blue line), CD19^{hi}IL-10^{+}(red line) and IL-10^{-} (dashed line) cells. CD19^{+} splenocytes were cultured with LPS, PMA, ionomycin and brefeldin A for 5 hr before staining for IL-10. (f) Flow cytometry histogram of TCF1 and LEF1 expression on CD19^{lo}IL-10^{+} (blue line), CD19^{hi}IL-10^{+}(red line) and IL-10^{-} (dashed line) subsets (left) and geometric mean fluorescence intensity (gMFI) quantification of TCF1 and LEF1(right). (g) Flow cytometry plots (left) and quantification of percentage (right) of CD19^{lo}IL-10^{+} (blue line), CD19^{hi}IL-10^{+} (red line) cells from TCF1^{WT}LEF1^{WT} and TCF1$^{\Delta}$LEF1$^{\Delta}$ mice. (h) Mean clinical score of mice treated with either PBS (open circles with dots) or peritoneal B-1 cells from TCF1^{WT}LEF1^{WT} (filled circles) and TCF1$^{\Delta}$LEF1$^{\Delta}$ (open circles) that had been treated with the TLR7/8 ligand R848 for 48 hr in vitro. Each symbol represents an individual mouse, Data are mean ± s.d. Data from one experiment with five or ten mice per genotype, representative of two independent experiments (c-f, g), Statistical analysis was performed using Mann-Whitney t test (e-h). *P < 0.05, **P < 0.001 and ***P < 0.0001.

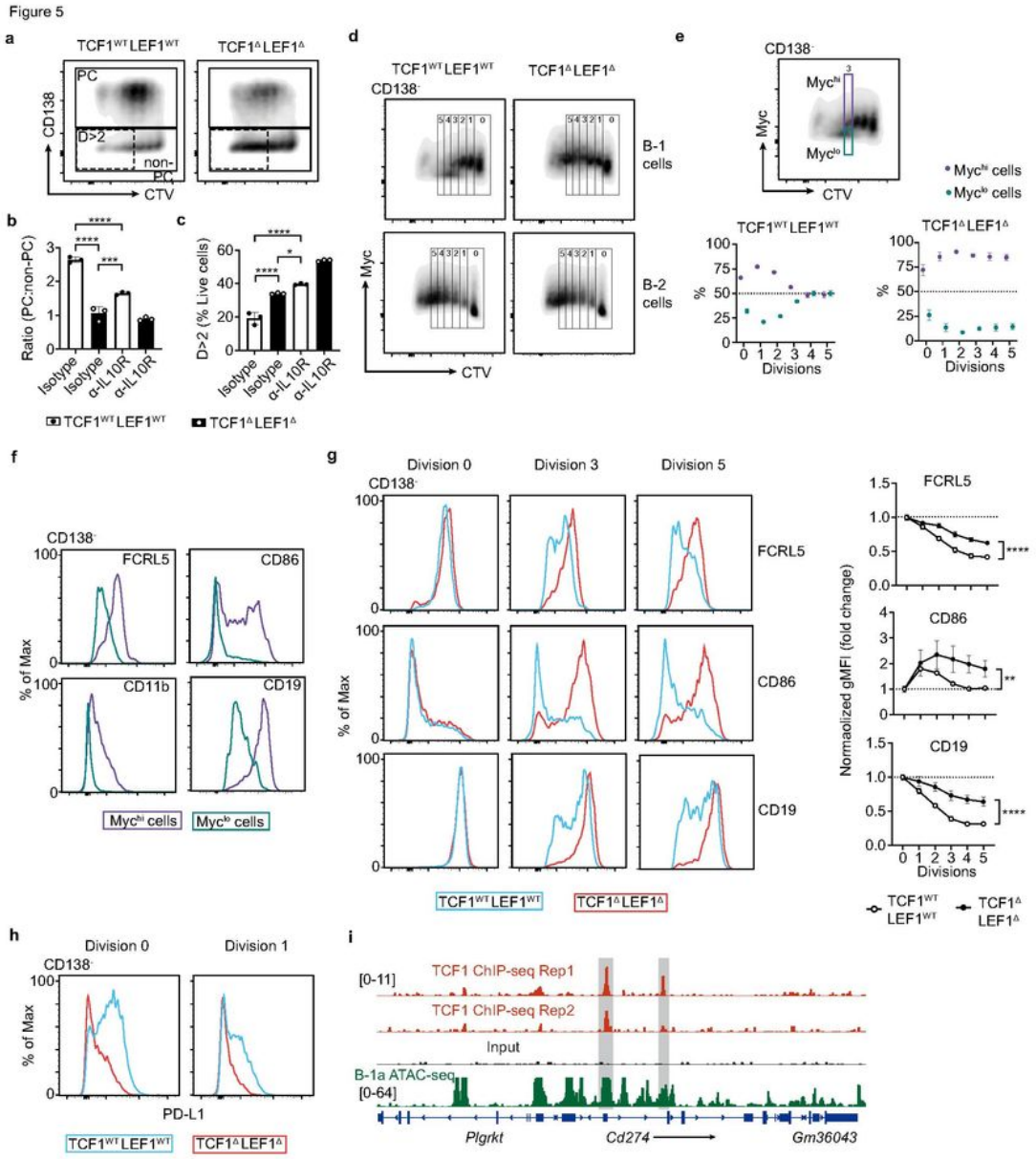

Figure 5

TCF1 and LEF1 deficiency B-1 cells increase proliferation after LPS stimulation. Magnetically purified peritoneal cavity TCF1^{WT}LEF1^{WT} or TCF1$^{\Delta}$LEF1$^{\Delta}$ B-1 cells were cultured with LPS and IgG1 isotype for 3 days. (a-b) Flow cytometry plots (a) and Quantification of mean ratio of PC (CD138^{+}) and non-PC (CD138^{-}) cells (b). (c) Quantification of percentage of cells after the second division in non-PC cells. (d) Representative flow cytometry plots of Myc expression through cell proliferation as measured by dilution

of CTV. (e) Representative gating strategy of Myc^{hi} and Myc^{lo} cells (upper) and Quantification of percentage of Myc^{hi} and Myc^{lo} in each division (bottom). (f) Representative histogram plots of CD86, FCRL5, CD11b and CD19 expression between Myc^{hi} and Myc^{lo} cells. (g) Representative histogram plots (left) and Quantification of fold change (right) of CD86, FCRL5, and CD19 expression on cells of undivided (D0), the third division (D3) and the fifth division (D5) on $TCF1^{WT}LEF1^{WT}$ or $TCF1^{\Delta}LEF1^{\Delta}$ B-1 cells stimulated with LPS for 3 days. (h) Representative histogram plots of PD-L1 expression in D0 and D1 of $TCF1^{WT}LEF1^{WT}$ or $TCF1^{\Delta}LEF1^{\Delta}$ B-1 cells stimulated with LPS for 3 days. (i) ChIP-seq analysis of TCF1 and LEF1 binding in $CD4^{+}CD8^{+}$ thymocytes and ATAC-seq analysis at *PD-L1* on B-1a cells from *Vh12/Vk4* transgenic mice . Data are mean ± s.d. Data are from one experiment representative of two independent experiment with a total of nine mice per genotype, peritoneal cavity cells from three mice are pooled together. Statistical analysis was performed using Statistical analysis was performed using parametric t test (b-d), Mann-Whitney t test (f). *$P < 0.05$, **$P < 0.001$ and ***$P < 0.0001$.

Supplementary Files

This is a list of supplementary files associated with this preprint. Click to download.

- ExtendedDataFiguresLegends.docx
- ExtendedFigures.pdf